Towards the two-loop electroweak corrections to the Drell-Yan process: the infrared structure

Tommaso Armadillo,[a,b] **Simone Devoto,**[c] **Michele Dradi,**[b] **Alessandro Vicini**[b,d]

[a]*Centre for Cosmology, Particle Physics and Phenomenology (CP3), Université catholique de Louvain, Chemin du Cyclotron, 2, B-1348 Louvain-la-Neuve, Belgium*

[b]*Dipartimento di Fisica "Aldo Pontremoli", University of Milano and INFN, Sezione di Milano, I-20133 Milano, Italy*

[c]*Department of Physics and Astronomy, Ghent University, 9000 Ghent, Belgium*

[d]*Tsung-Dao Lee Institute, Shanghai Jiao Tong University, Shanghai, 200120, China*

E-mail: tommaso.armadillo@uclouvain.be, simone.devoto@ugent.be, michele.dradi@mi.infn.it, alessandro.vicini@mi.infn.it

ABSTRACT: We discuss the lepton-pair production process in Quantum Electrodynamics. We present the ultraviolet-renormalised and infrared-subtracted finite contribution of the second-order virtual corrections to the inclusive lepton-pair production cross section $u\bar{u} \to e^+e^-$. The results are obtained within a new computational framework, OCEANN, developed in view of the evaluation of the exact two-loop electroweak virtual corrections to high-energy scattering processes. One of the key methodological features in this approach is the representation of the scattering amplitude with arbitrary precision at every stage of the calculation. The analysis in QED allows us to address the treatment of the infrared structure of the process and it can be easily extended to the complete electroweak Standard Model case. The perfect agreement with the literature, for this subset of corrections, provides a non trivial validation of the general framework.

KEYWORDS: QED, Multi-loop calculations

Contents

1 Introduction

The hadro-production of lepton-antilepton or lepton-antineutrino pairs, known respectively as neutral current (NC) and charged current (CC) Drell-Yan (DY) processes [1], is crucial at hadron colliders since it provides the environment for a precise study of the gauge sector of the Standard Model (SM) of the electroweak (EW) and strong interactions. In particular, the NC DY process is important for the determination of the Z-boson mass and the effective weak mixing angle, and the CC DY process is important for the determination of the W-boson mass. These three EW parameters are known at the moment with small relative errors, 0.01% for the boson masses and 0.1% for the effective weak mixing angle [2–6], estimated within a fitting procedure of the measured kinematical distributions of the final state leptons with corresponding theoretical templates [7–12]. The searches for new heavy particles, beyond those predicted by the SM, can be performed with the DY observables, exploring the few TeV regime. The prospects in the High-Luminosity phase of the LHC (HL-LHC) are extremely promising, with a statistical error below the 1% level for invariant masses of about 1 TeV, which will allow a test of the theory predictions at the quantum level. Due to the high precision of the experimental data, any statistically

meaningful comparison requires correspondingly precise theoretical predictions, which must include higher-order perturbative corrections.

The region of large invariant mass of the lepton pair is well understood from the point of view of the strong interactions, after the completion of the calculation of the third order corrections in Quantum Chromodynamics (QCD) [13–15]. The large size of the Next-To-Leading Order (NLO) EW [16–25] corrections, and in turn of the Next-To-Next-To-Leading Order (NNLO) mixed QCD-EW corrections [26–28], suggests that also the NNLO EW effects might potentially be large, at the several percent level, as it appears for instance in [29, 30]. If confirmed, effects of this size could not be neglected for a meaningful comparison with the experimental data. In a complementary perspective, the residual uncertainties of a NLO-EW calculation of the NC DY process, due to renormalisation ambiguities, range between 1 and 10% in the TeV region, with a strong limitation of the discovery potential of any signal of physics beyond the SM [31], based on current tools. The NNLO-EW corrections will also be relevant for precision phenomenology at HL-LHC in the 80-400 GeV interval, where sub-percent errors are expected. All these remarks motivate a thorough investigation of this set of quantum effects, which represents, on the other hand, a major theoretical and computational challenge.

The DY process has always represented, in the study of the QCD and EW interactions, a benchmark: for its physical relevance and also for the challenges in the development of new computational techniques of higher-order quantum corrections. A major progress has been witnessed in QCD, spanning four decades, with the development of new mathematical tools to compute the Feynman integrals and to evaluate the scattering amplitudes for the production of a colorless final state, involving massless partons up to third perturbative order, both at inclusive and differential level, possibly with the inclusion, beyond the fixed-order results, of the resummation of logarithmically enhanced terms to all orders in the coupling constant expansion [13–15, 32–54]. The progress for the first order EW corrections is comparatively more recent: while the one-loop Feynman integrals are well established [55], the development of several tools for the automated generation of the scattering amplitudes [56–58] allows to study arbitrary processes, despite the large size of the analytical expression of the amplitude, the latter due to the presence of several different masses of the gauge and Higgs bosons and of the fermions. The combination of the difficulties in the amplitude generation and in the evaluation of the Feynman integrals relevant for the NNLO mixed QCD-EW corrections have been faced in steps of increasing complexity, first considering the combination of first order QCD and EW corrections in Monte Carlo simulation tools [31, 59–64], then studying in detail the resonant production of a gauge boson [65–76], and eventually with the discussion of the complete amplitude for the production of a lepton pair [26–28, 77–82]. New techniques based on the series expansion solution of the differential equations satisfied by the so called Master Integrals (MIs) have opened the way to the evaluation of a general Feynman integral with an arbitrary set of internal complex valued masses [83–88].

The evaluation of the NNLO EW corrections to the cross section $\sigma(pp \to \ell^+\ell^- + X)$ is a formidable challenge, which deserves the development of a dedicated computational framework, where all the different conceptual and computational issues relevant in the

calculation are addressed in a fully consistent way. We introduce here `OCEANN` (Organised Calculation of Electroweak Amplitudes at NNLO), a framework that combines the usage of different existing tools and allows an experienced user to perform a full two-loop EW calculation in a systematic and sustainable way. The challenge is evident in the evaluation of all the contributions to the inclusive cross section, because of the high target precision in the evaluation of the subprocesses where the lepton pair is accompanied by real radiation, but also and foremost because of the complexity of the two-loop virtual corrections to the lowest order partonic subprocesses. Several distinct physics items have to be discussed for the latter: the ultraviolet (UV) renormalisation in the presence of unstable particles and the description of the gauge boson resonances; the evaluation of the Feynman integrals with internal complex-valued masses; the corrections due to an internal closed fermionic loop and the study of the couplings of the gauge bosons to fermions; the subtraction of all the infrared (IR) divergences due to the emission of photons; the identification of the corrections due to massive weak bosons, which have a soft logarithmic behavior in the high-energy limit. Each of these items raises specific mathematical and computational issues, which deserve a detailed discussion.

The main methodological choice that defines the `OCEANN` framework is that all the elements contributing to the expression of the scattering amplitude are evaluated with arbitrary numerical precision, an approach ideally suited for the calculation of higher-order EW corrections. In the QCD literature, the cancellation of the divergent terms, which appear in the UV renormalisation and in the subtraction of the IR divergences, is typically achieved at symbolical level, with the coefficients written as exact numbers. However, this is not necessarily viable at the two-loop QCD-EW or purely EW level, because of the presence of new kinds of integrals, whose solution is not known in closed form. Nevertheless, the series expansion approach implemented within `OCEANN` allows for an evaluation of such integrals with arbitrary numerical precision. This feature guarantees the exactness of the cancellation of the divergent terms, also in the most difficult cases. The same approach naturally applies to all the integrals present in a full two-loop EW calculation, including those whose solution is still unknown in the literature. Furthermore, embedding the calculation in a framework leads to a uniform treatment and bookkeeping of all the integrals which appear in the scattering amplitude, a feature which is particularly convenient in view of an advanced automation of the calculation and deployment on large computing clusters.

In this paper we focus on the IR structure of the virtual amplitudes. The universality of the IR divergences (cfr. [89] and references therein) allows a complete explicit discussion of this topic in a slightly simplified framework: we present here the two-loop virtual corrections to the production of a massive lepton pair in quark-antiquark annihilation, and for the sake of definiteness we consider $u\bar{u} \rightarrow e^+e^-$, in QED, including the UV renormalisation and the subtraction of the IR divergences. The discussion of the NNLO QED corrections in QED to the scattering of 2 fermions into 2 fermions is mature in the literature [90–96] and a renovated interest has lead to a closed form representation of the two-loop amplitudes [97, 98]. The latter results are an important benchmark for the validation of our computational framework and to demonstrate its readiness to the evaluation of the two-loop EW

corrections.

The paper is organised in the following way. In Section 2, we describe the general properties of the IR divergences in high-energy scattering processes and our subtraction formalism. In Section 3 we detail our case study, namely the evaluation of the two-loop virtual amplitude for the process $u\bar{u} \to e^+ e^-$ in QED, including some details of the UV renormalisation. In Section 4 we comment on the workflow implemented in OCEANN to increase the level of automation in the evaluation of two-loop EW corrections, we give an explicit example with the two-loop virtual corrections in QED, and we demonstrate the numerical control on the cancellation of UV and IR divergences. Finally, in Section 5 we draw our conclusions.

2 Infrared Singularities and Universal Pole Structure

The bare amplitude $\hat{\mathcal{M}}$ for an arbitrary scattering process can be expressed in terms of a series expansion in the unrenormalised strong ($\hat{\alpha}_S$) and electroweak ($\hat{\alpha}$) coupling constants,

$$|\hat{\mathcal{M}}\rangle = 4\pi\hat{\alpha} \sum_{i,j} \left(\frac{\hat{\alpha}_s}{4\pi}\right)^i \left(\frac{\hat{\alpha}}{4\pi}\right)^j |\hat{\mathcal{M}}^{(i,j)}\rangle \, . \tag{2.1}$$

Despite the full generality of Equation (2.1), the IR divergent structure of the bare amplitude $\hat{\mathcal{M}}$ can be captured in a process-independent way by exploiting the universal structure of IR divergences [89]. This is made possible, after the UV renormalisation[1], by the introduction of suitable subtraction operators $\mathcal{I}^{(i,j)}$, which allow to write at each perturbative order the finite contribution of the amplitude, $|\mathcal{M}^{(i,j),fin}\rangle$, with the follow iterative definition, where $|\mathcal{M}^{(0,0)}\rangle$ is the lowest-order amplitude:

$$|\mathcal{M}^{(0,0),fin}\rangle = |\mathcal{M}^{(0,0)}\rangle \, , \tag{2.2}$$

$$|\mathcal{M}^{(i,j),fin}\rangle = |\mathcal{M}^{(i,j)}\rangle - \sum_{k=0}^{i}\sum_{l=0}^{j} \mathcal{I}^{(k,l)} |\mathcal{M}^{(i-k,j-l),fin}\rangle \, . \tag{2.3}$$

The operators $\mathcal{I}^{(i,j)}$ describe the emission of massless gauge bosons such as gluons and photons and the production of additional light fermion pairs. The scattering amplitude diverges when the emitted particles have vanishing energy (soft limit) or form a vanishing angle with their emitter (collinear limit). The integration over the real phase space of the emitted particles, or in the case of virtual corrections the integration over the loop momentum, are divergent and we regularise them working in $d = 4 - 2\epsilon$ space-time dimensions. The divergences appear as poles in ϵ. In the case of emissions off the massive final state, the emitter mass m acts as a natural regulator, the collinear divergence represented by a $1/\epsilon$ pole is absent, but in the amplitude we find logarithms of m. Dimensional regularization is adopted also to discuss the UV renormalisation. In the case of EW corrections, the conservation of the vector current implies that the impact of genuinely weak corrections exactly vanishes in the divergent emission factors, whose expression receives only QED

---

[1]We use symbols without a hat to describe the UV renormalised quantities.

contributions. The universality of the IR divergent factors implies that their expression depends only on the identity of the external particles of the scattering under study, but not on the details of the hard interaction; in other words, the discussion of the IR structure of the $u\bar{u} \to e^+e^-$ process is the same, irrespective of the fact that we have a QED or an EW interaction driving the scattering process.

Considering the case of QED corrections up to second order, Equation (2.3) takes the form

$$|\mathcal{M}^{(0,1),fin}\rangle = |\mathcal{M}^{(0,1)}\rangle - \mathcal{I}^{(0,1)}|\mathcal{M}^{(0,0)}\rangle \tag{2.4}$$

$$|\mathcal{M}^{(0,2),fin}\rangle = |\mathcal{M}^{(0,2)}\rangle - \mathcal{I}^{(0,2)}|\mathcal{M}^{(0,0)}\rangle - \mathcal{I}^{(0,1)}|\mathcal{M}^{(0,1),fin}\rangle . \tag{2.5}$$

We restrict the discussion to the pure QED corrections to a scattering process $2 \to n$, where the final state only contains massive emitters. In this case, the infrared structure of the amplitude is encapsulated in the subtraction operators $\mathcal{I}^{(0,1)}$ and $\mathcal{I}^{(0,2)}$, defined as

$$\frac{1}{S_\epsilon} \mathcal{I}^{(0,1)} = \frac{\Gamma_0'}{4\epsilon^2} + \frac{\Gamma_0}{2\epsilon} , \tag{2.6}$$

$$\frac{1}{S_\epsilon^2} \mathcal{I}^{(0,2)} = \frac{(\Gamma_0')^2}{32\epsilon^4} + \frac{\Gamma_0'}{8\epsilon^3}\left(\Gamma_0 - \frac{3}{2}\beta_0\right) + \frac{\Gamma_0}{8\epsilon^2}\left(\Gamma_0 - 2\beta_0\right) + \frac{\Gamma_1'}{16\epsilon^2} + \frac{\Gamma_1}{4\epsilon} - \frac{2}{3}\sum_k^{\text{massive}} n_k q_k^2 \tag{2.7}$$

$$\times \left\{ \frac{1}{2\epsilon^2}\Gamma_0' \log\left(\frac{\mu_R^2}{m_k^2}\right) + \frac{1}{4\epsilon}\left[\Gamma_0'\left(\log^2\left(\frac{\mu_R^2}{m_k^2}\right) + \frac{\pi^2}{6}\right) + 4\Gamma_0 \log\left(\frac{\mu_R^2}{m_k^2}\right)\right]\right\} ,$$

where $S_\epsilon = (4\pi e^{-\gamma_E})^\epsilon$ and μ_R is the renormalisation scale. The structure of the subtraction operators is governed by the functions Γ and Γ', which can be obtained from the abelianisation of the QCD soft and cusp anomalous dimensions [99, 100]

$$\Gamma = \sum_i \gamma_l^i + Q_1 Q_2 \gamma^{\text{cusp}}(\alpha) \log\left(\frac{\mu_R^2}{-2p_1 \cdot p_2}\right) \tag{2.8}$$

$$+ \sum_j \gamma_h^j - \sum_{j_1 \neq j_2} \frac{Q_{j_1} Q_{j_2}}{2} \gamma^{\text{cusp}}(\alpha)\beta_{j_1,j_2} \coth\beta_{j_1,j_2}$$

$$- \sum_{i,j} Q_i Q_j \gamma^{\text{cusp}}(\alpha) \log\left(\frac{\mu_R m_j}{2p_i \cdot p_j}\right) ,$$

$$\Gamma' = -\sum_i Q_i^2 \gamma^{\text{cusp}}(\alpha) , \tag{2.9}$$

$$\gamma^{\text{cusp}}(\alpha) = \frac{\alpha}{4\pi}\left[4 - \frac{80}{9}\left(\frac{\alpha}{4\pi}\right)\sum_k^{\text{massless}} n_k q_k^2 + \mathcal{O}(\alpha^3)\right] . \tag{2.10}$$

We refer to massless initial state particles, with momentum p_i and electric charge Q_i, while with the labels $j = 3, \ldots, n$ we refer to the massive final state emitters, with mass m_j, momentum p_j and electric charge Q_j. The first line of Equation (2.8) thus represents the contribution coming from initial-state radiation, with γ_l^i defined as

$$\gamma_l^i = \frac{\alpha}{4\pi}Q_i^2\left\{-3 + \left(\frac{\alpha}{4\pi}\right)\left[Q_i^2\left(-\frac{3}{2} + 2\pi^2 - 24\zeta_3\right) + \left(\frac{130}{27} + \frac{2\pi^2}{3}\right)\sum_k^{\text{massless}} n_k q_k^2\right] + \mathcal{O}(\alpha^3)\right\} . \tag{2.11}$$

In Equation (2.11) the sum runs over the particles considered massless in the computation, with multiplicity n_k (3 for the coloured quarks, 1 for the leptons) and electric charge q_k, giving the contribution of the soft and collinear emission of light fermion pairs from the initial-state partons. The second line of Equation (2.8) instead contains the contribution coming from the final-state particles, with γ_h^j defined as

$$\gamma_h^j = \frac{\alpha}{4\pi} Q_j^2 \left[-2 + \left(\frac{\alpha}{4\pi} \right) \frac{40}{9} \sum_k^{\text{massless}} n_k q_k^2 + \mathcal{O}(\alpha^3) \right] . \tag{2.12}$$

Finally, the third line of Equation (2.8) contains the interference between initial-state and final-state emissions. We label with β_{j_1,j_2} the function defined by the relation

$$\cosh \beta_{j_1,j_2} = -\frac{p_{j_1} \cdot p_{j_2}}{m_{j_1} m_{j_2}} . \tag{2.13}$$

The physically allowed values for $\cosh \beta_{j_1,j_2}$ with j_1 and j_2 outgoing are $\cosh \beta_{j_1,j_2} \leq 1$, corresponding to $\beta_{j_1,j_2} = -b + i\pi$ with real $b \geq 0$.

The symbols Γ_n, Γ_n' in Equation (2.6, 2.7) indicate the coefficients of the series expansion in the weak coupling α of the corresponding anomalous dimensions

$$\Gamma^{(\prime)} = \sum_{n \geq 0} \left(\frac{\alpha}{4\pi} \right)^{n+1} \Gamma_n^{(\prime)} . \tag{2.14}$$

The sum in Equation (2.7) takes care of the collinear emission of massive fermion pairs and of soft emission with a massive quark loop. As such, it runs over all the particles k with electric charge q_k considered with a non-zero mass m_k in the calculation.

The expression of $\mathcal{I}^{(0,2)}$ receives a contribution from the renormalisation of the one-photon emission vertex, which has been performed in the $\overline{MS}$ scheme, and contributes with a β_0 term

$$\beta_0 = -\frac{4}{3} \sum_k^{\text{massless}} n_k q_k^2 . \tag{2.15}$$

The expressions in Eqs. (2.6, 2.7) are fully consistent with those presented in [97], and have been derived with the abelianization of the QCD subtraction operator presented in [99, 101, 102].

3 Two-loop corrections to lepton-pair production in QED

3.1 The process

The process under study is the production of a pair of massive leptons in quark-antiquark annihilation, for the sake of definiteness an up-quark pair annihilating into an electron pair

$$u(p_1) + \bar{u}(p_2) \rightarrow e^+(p_3) + e^-(p_4) . \tag{3.1}$$
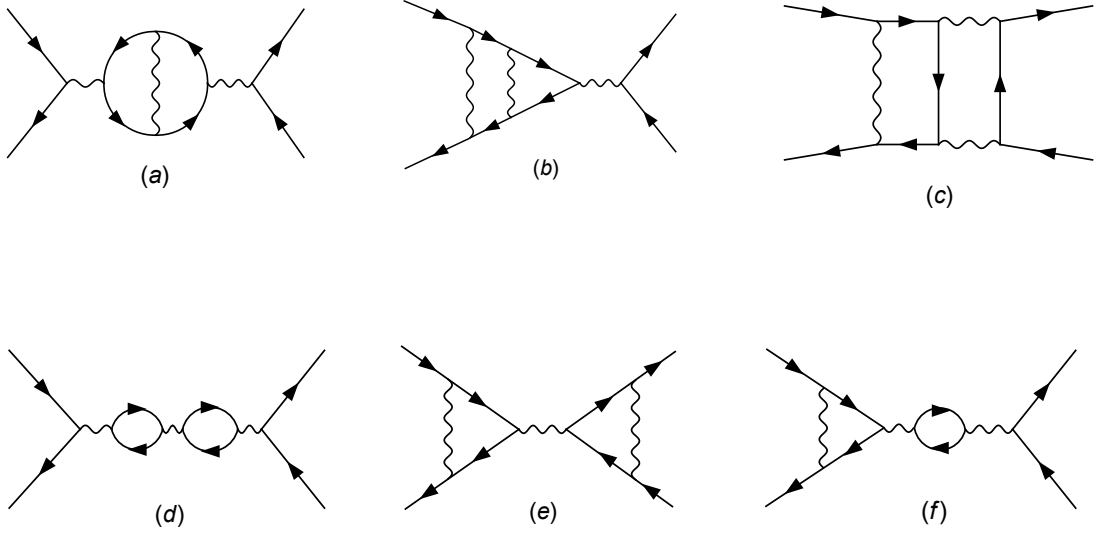
Figure 1. Sample two-loop Feynman diagrams: 1-particle irreducible and factorisable one-loop ×one-loop contributions.

The electron mass is labeled by m_e. The Mandelstam variables are defined as

$$s = (p_1 + p_2)^2, \ \ t = (p_1 - p_3)^2, \ \ u = (p_2 - p_3)^2 \ \text{ with } s + t + u = 2m_e^2, \qquad (3.2)$$

while the on-shell conditions of the external particles are

$$p_1^2 = p_2^2 = 0; \quad p_3^2 = p_4^2 = m_e^2. \qquad (3.3)$$

In this paper we plan to study the IR structure of the second order purely EW corrections to this process, and to achieve this goal we limit the discussion to the evaluation in QED of the interference terms[2]

$$\langle \hat{\mathcal{M}}^{(0,0)} | \hat{\mathcal{M}}^{(0,1)} \rangle, \ \ \langle \hat{\mathcal{M}}^{(0,0)} | \hat{\mathcal{M}}^{(0,2)} \rangle, \qquad (3.4)$$

which contribute to the corrections to the unpolarised squared matrix element of the process in Equation (3.1), at $\mathcal{O}(\alpha^2)$. The evaluation of the finite part of the two-loop virtual amplitude entails first the discussion of the UV renormalisation, followed by the subtraction of the IR divergences.

In Figure 1 are presented some examples of two-loop Feynman diagrams contributing to the bare interference term $\langle \hat{\mathcal{M}}^{(0,0)} | \hat{\mathcal{M}}^{(0,2)} \rangle$. (a), (b), (c) are sample diagrams for each 1-particle irreducible (1PI) category in which we can group the diagrams, respectively self-energies, vertices and boxes 1PI diagrams. In contrast, (d), (e), (f) represent

---

[2]We do not discuss the interference term $\langle \hat{\mathcal{M}}^{(0,1)} | \hat{\mathcal{M}}^{(0,1)} \rangle$, also contributing at $\mathcal{O}(\alpha^2)$, which can be easily obtained with any NLO amplitude generator.

sample diagrams for the factorisable contributions given by the iteration of 2 one-loop diagrammatic corrections. The cancellation of the UV divergences stemming from the bare diagrams follows according to a standard renormalisation procedure. The resulting amplitudes are expressed in terms of renormalised parameters, in turn related to measurable quantities. We write the UV-renormalised amplitude as a Laurent expansion in ϵ, and we keep only terms up to $\mathcal{O}(\epsilon^2)$ or $\mathcal{O}(\epsilon^0)$, at one- or two-loop respectively, in order to include all the second-order finite contributions when we perform the IR subtraction described in Section 2.

3.2 Ultraviolet renormalisation

The SM renormalisation up to second order in the electroweak interaction has been discussed in [103–108] both for the on-shell and the $\overline{MS}$ renormalisation scheme. The electric charge renormalisation at $\mathcal{O}(\alpha^2)$ has been presented in detail in [109] while in [97] it is possible to find the analytical expressions of the fermion mass and wave-function counterterms in QED for the case of one internal mass. Our renormalisation procedure within OCEANN is realized with a dedicated semi-analytical evaluation of the coupling and fermions renormalisation constants, whose definitions follow from the 2-point Green functions of the theory and can be found in Appendix A. The generalisation of this computational approach to the complete two-loop EW case is straightforward.

We write the virtual amplitude for the production of a pair of massive electrons as

$$|\hat{\mathcal{M}}(u\bar{u} \to e^+e^-)\rangle = 4\pi\hat{\alpha} \sum_{j=0}^{\infty} \left(\frac{\hat{\alpha}}{4\pi}\right)^j |\hat{\mathcal{M}}^{(0,j)}(s,t,\hat{m}_e,\hat{m}_f)\rangle , \qquad (3.5)$$

where $|\hat{\mathcal{M}}^{(0,j)}\rangle$ is the bare amplitude at j^{th} perturbative order in $\hat{\alpha}$, and all the parameters (the electric charge $\hat{e}$, the electron mass $\hat{m}_e$ and the mass $\hat{m}_f$ of a generic fermion f) and fields are treated as bare quantities, labeled with a hat. The renormalised amplitude is obtained by the replacement of all the bare quantities with their renormalised counterparts: $\hat{e} \to e + \delta e$, $\hat{m}_e \to m_e + \delta m_e$, $\hat{m}_f \to m_f + \delta m_f$, and the rescaling $\hat{\psi} \to Z_{\psi}^{\frac{1}{2}}\psi = (1 + \delta Z_{\psi})^{\frac{1}{2}}\psi$ for each external fermionic field, where we consider $\hat{\alpha} = \hat{e}^2/(4\pi)$ and $\alpha = e^2/(4\pi)$,

$$
\begin{aligned}
|\mathcal{M}(u\bar{u} \to e^+e^-)\rangle &= Z_u^{\frac{1}{2}} Z_{\bar{u}}^{\frac{1}{2}} Z_{e^+}^{\frac{1}{2}} Z_{e^-}^{\frac{1}{2}} \ 16\pi^2 \times \\
&\quad \sum_{j=0}^{\infty} \left(\frac{e+\delta e}{4\pi}\right)^{2j+2} |\hat{\mathcal{M}}^{(0,j)}(s,t,m_e+\delta m_e, m_f+\delta m_f)\rangle \\
&= 4\pi\alpha \sum_{j=0}^{\infty} \left(\frac{\alpha}{4\pi}\right)^j |\mathcal{M}^{(0,j)}(s,t,m_e,m_f)\rangle .
\end{aligned}
\qquad (3.6)
$$

Since not only the bare amplitude, but also the counterterms are computed in perturbation theory, we expand the renormalised amplitude and collect all the terms of the same order in the coupling constant, checking the cancellation of the UV divergences. The result can be eventually cast as an expansion in the renormalised coupling α, where $|\mathcal{M}^{(0,j)}\rangle$ includes diagrammatic and counterterm contributions and is UV finite.
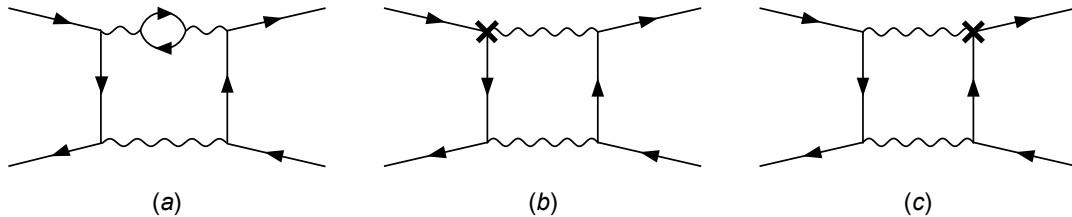
Figure 2. Sample Feynman diagrams with the insertion of a closed fermionic loop along a photon line and the associated electric charge counterterm diagrams.

At first order, we identify three subsets of Feynman diagrams, the corrections to the tree-level photon propagator, the initial (final) vertex corrections and the associated wave function (WF) factors on the external quark (electron) lines, the box diagrams. Each of these three groups of diagrams is UV finite, after the inclusion of the one-loop counterterms: the boxes are UV finite by power counting, the photon vacuum polarization is by construction made finite by the electric charge counterterm; the Ward identities guarantee the UV finiteness of the combination of the vertex corrections with the WF constants of the corresponding external lines. Additional poles in the dimensional regularization parameter ϵ are however still present, because of the IR divergent behaviour of the vertex and box corrections.

At the second perturbative order, the finiteness of the self-energy corrections to the tree-level photon propagator follows from the definition of the electric charge counterterm, once all the factorisable one-loop contributions have been properly included. Like in the one-loop case, the UV-finiteness of the sum of vertex and WF contributions can not be directly checked, because of the presence of IR poles, also expressed with the regulator ϵ. We identify two distinct groups of second-order 1PI diagrams: those with the exchange of two internal photons (like for instance diagrams (*b*) and (*c*) in Figure 1), and those with the insertion, along an internal photon line of a one-loop diagram, of a closed fermionic loop (like for instance diagram (*a*) in Figure 2). The latter features an UV divergence which is subtracted by the one-loop electric charge counterterm applied to the corresponding one-loop amplitude (diagrams (*b*) and (*c*) in Figure 2).

Since the IR subtraction terms discussed in Section 2 have been derived in the $\overline{MS}$ renormalisation scheme for the electric charge, we have to adopt it also in the evaluation of the virtual corrections to ensure a consistent cancellation of the IR divergencies. While our final result will thus be expressed in terms of the coupling coupling $\alpha_{\overline{MS}}(\mu_R)$, evaluated at the renormalisation scale μ_R, it can also be expressed in terms of the on-shell fine structure constant $\alpha(0)$, with a finite renormalisation at the end of the calculation, as it is discussed in detail in Section 4.3. The fermion masses and the fermion wave-function counterterms are instead always computed in the on-shell scheme.

We remark that a change in the electric charge renormalisation scheme has a non trivial

impact on the pattern of the subtraction of the IR poles. If we consider as an example the two diagrams (*b*) and (*c*) in Figure 2, we can easily recognize the fact that a finite additional contribution to the counterterm insertion is a constant which multiplies the entire underlying one-loop diagram. The latter features soft and collinear IR poles, which are multiplied by this additional factor. The cancellation of these extra poles is possible only with a corresponding contribution from the real emission diagrams, or equivalently from the subtraction term.

4   Results

The calculation presented in this paper illustrates with a non trivial example the application of `OCEANN`, a new complete workflow for the evaluation of two-loop EW corrections. It provides in particular the validation of a new semi-analytical approach to handle the cancellation of UV and IR divergences, represented by poles in dimensional regularization.

4.1   Automatic generation and evaluation of the two-loop virtual corrections

The computational framework `OCEANN` is a collection of codes and packages that provides, to an experienced user, all the necessary tools to face the challenges of the calculation of a multi-loop electroweak amplitude in a consistent way. The main steps of these computations are: the calculation of the squared matrix element which contains all the interference terms between the Feynman diagrams that contribute to the process; the evaluation of the Feynman loop integrals present in the amplitude; and, finally, the cancellation of the UV and IR divergences via the renormalisation and subtraction procedures.

   The evaluation of the squared matrix elements is implemented, within `OCEANN`, in the Mathematica package `Abiss` (Amplitudes Builder, Interference Solver and Simplifier). `Abiss` expresses the final result as a combination of MIs, each multiplied by a rational function of the kinematical invariants and masses of the process, with a workflow which can be described schematically by the following points:

1. The generation of the Feynman diagrams of the chosen scattering process is performed with `FeynArts` [110], which supports several model files for the SM and its extensions.

2. The Feynman diagram with the insertion of UV counterterms are generated with a custom model file for `FeynArts` which provides the counterterms in symbolical form. Their numerical values, as a Laurent series in the dimensional regularization parameter ϵ, can be computed together with all the other diagrams, or they can be read from any external counterterm library.

3. The evaluation of the interference between an amplitude and its hermitian conjugate[3], including the sum over all the external polarizations, is performed by dedicated routines in `Abiss`. The result is a list of expressions, Lorentz scalars, including Feynman loop integrals and coefficients, functions of kinematical invariants and masses.

---

[3]We can in full generality consider an amplitude and a projector.

4. All the Feynman integrals are classified in terms of integral families. The user can propose a preferred choice of integral families, in terms of which `Abiss` tries to write all the Feynman integrals present in the computation[4]. If the assignment of a given Feynman integral to one of the available families is not possible, `Abiss` automatically completes the tentative set, using the information of the new Feynman integral to introduce the new family. At the end of this classification step, the initial information relevant for the reduction to a minimal set of so called MIs is available and automatically organized in a group of dedicated directories.

5. The output of the previous point is ready for the external run of any code able to generate all the relations useful to express a generic element of an integral family as a linear combination of MIs. Such relations include IBP and Lorentz identities. Within `OCEANN`, we consider as reference code for this task `KIRA` [111–114]. The outcome of the run can be imported back to the directories already set-up by `Abiss`.

6. With the help of the reduction rules computed in the previous point, `Abiss` is able to organize the squared matrix element as a sum over the N_{MI} MIs $\mathcal{I}_j$, with appropriate coefficients c_j. For example, in the case of the two-loop contributions,

$$\langle \mathcal{M}^{(0)} | \mathcal{M}^{(0,2)} \rangle = \sum_{j=1}^{N_{MI}} c_j \, \mathcal{I}_j \, . \tag{4.1}$$

Both coefficients and integrals depend on the kinematical invariants and on the masses of the particles of the model.

The evaluation of the MIs which have been identified in the first stage is handled within `OCEANN` with the public Mathematica package `SeaSyde` [85, 88], following a simple workflow:

1. For each integral family, we compute the systems of differential equations satisfied by its MIs, with respect to the kinematical invariants. For this task, several tools are publicly available, like e.g. `LiteRed` [115] or `REDUZE` [116].

2. We compute the boundary condition values for each MI with the code `AMFlow` [86].

3. We solve the system of differential equations with `SeaSyde`.

`SeaSyde` solves the system of differential equations with the series expansion procedure [83, 84]. The solution is studied in the complex plane, with an original algorithm for the analytical continuation of the solutions. The efficient evaluation of a series of points in one single run is relevant for the preparation of numerical grids which sample the whole phase space of the process. The numerical results have arbitrary precision, which can be selected by the user and is achieved with an appropriate number of terms in the power series used to represent the solution.

---

[4]Different routings of the loop momenta and trivial symmetry relations are tested, to match the momenta with those of the definition of the integral family.

The last steps of the calculation are handled by internal routines within `OCEANN`: the combination of the diagrammatic and counterterm contributions, to achieve the UV finiteness of the amplitude; the subtraction of the IR poles from the UV renormalised interference terms, according to the strategy described in Section 2. The sequences of points, covering the whole phase space, computed by Seasyde for the MIs and within `Abiss` for their rational coefficients, express the finite contribution of the virtual corrections, relevant for phenomenological studies. One possible strategy is the preparation of grids which allow the evaluation of the correction at any phase-space point via interpolation, with excellent accuracy, in negligible time. This approach has been applied, for example, in the context of the mixed QCDxEW corrections in [28, 78].

The sequence of computational steps described above, taking place within the `OCEANN` framework, is fully general and applies to the evaluation of the squared matrix element of an arbitrary scattering process at a given perturbative order.

4.2 Explicit QED results and control over the cancellation of the IR poles

In the following, we present our results for the squared two-loop QED virtual amplitudes $\langle \mathcal{M}^{(0)} | \mathcal{M}^{(0,2)} \rangle$ for the process $u\bar{u} \to e^+ e^-$. We identify in total 11 families relevant for the description of two-loop box topologies[5]. In the classification of the vertex corrections we identify 6 new families, while in the analysis of the self-energy diagrams we find 2 new families.

The fully diagrammatic approach allows us to perform intermediate checks of the calculation. We find a finite result for the self-energy corrections to the tree-level photon propagator, after the introduction of the one- and two-loop electric charge counterterms. We check the cancellation of one pole in ϵ, when we combine a two-loop diagram with one fermion loop insertion together with the charge renormalisation of the adjacent vertices in the corresponding one-loop diagram.

The UV-renormalised results described in the previous Section still feature IR divergences, which appear as poles in the dimensional regularization parameter ϵ, but also as logarithms of the lepton mass in the case of the final state collinear divergences. It is a Laurent series in the dimensional regularization parameter, and the coefficients of the various powers of ϵ are numbers with arbitrary precision. In Table 1 we present the value of the coefficients of the different powers of ϵ, for the diagrammatic part and for the the two contributions to the subtraction operator, factorising the one-loop and Born squared amplitudes respectively. These results are obtained using the following values for the masses and Mandelstam invariants:

|	
$s = 10000 \text{ GeV}^2$	$m_e = 0.510998 \text{ MeV}$
$t = -2500 \text{ GeV}^2$	$m_\mu = 0.10566 \text{ GeV}$
$\mu_R = m_Z = 91.1535 \text{ GeV}$	$m_\tau = 1.77686 \text{ GeV}$
	$m_t = 172.69 \text{ GeV}$

---

[5]We count only once the insertion of a closed fermionic loop, treating the fermion mass as one generic parameter.

ϵ^{-4}	0.438 957 476 012 852 250 408 920 432 150 96
	−0.438 957 476 012 852 250 408 920 432 150 96
	0
ϵ^{-3}	−50.507 936 715 422 813 794 673 578 353 212
	50.507 936 715 422 813 794 673 578 353 212
	0
ϵ^{-2}	729.673 397 464 406 823 805 401 840 608 83
	−1334.179 413 878 226 352 371 754 281 425 92
	604.506 016 413 819 528 566 352 440 817 09
ϵ^{-1}	26 528.662 344 660 489 566 812 058 589 673 55
	−463.090 234 187 259 379 447 239 209 073 69
	−26 065.572 110 473 230 187 364 819 380 599 86
ϵ^{0}	401 847.447 345 130 812 729 654 039 382 635 2
	4376.812 767 994 162 824 254 022 583 940 2
	−308 980.388 535 504 055 198 013 748 925 268 4
$2\mathrm{Re}\langle\mathcal{M}^{(0,0)}|\mathcal{M}^{(0,2),fin}\rangle$	97 243.871 577 620 920 355 894 313 041 307 0

Table 1. Numerical coefficient, computed with at least 32 significant digits, of the IR poles present in the different contributions to Equation (2.5), for $s = 10000$ GeV^2 and $t = -2500$ GeV^2. For each pole, the first row refers to $2\mathrm{Re}\langle\mathcal{M}^{(0,0)}|\mathcal{M}^{(0,2)}\rangle$, the second one to $-\mathcal{I}^{(0,2)}\ 2\mathrm{Re}\langle\mathcal{M}^{(0,0)}|\mathcal{M}^{(0,0)}\rangle$ and the third one to $-\mathcal{I}^{(0,1)}\ 2\mathrm{Re}\langle\mathcal{M}^{(0,0)}|\mathcal{M}^{(0,1),fin}\rangle$. The last row is the final result of $2\mathrm{Re}\langle\mathcal{M}^{(0,0)}|\mathcal{M}^{(0,2),fin}\rangle$.

In the evaluation of the individual contributions to the amplitude, we encounter some terms whose value is several orders of magnitude larger than 1; we can inspect them all in absolute value and define $Q = \log_{10}(x)$, with x the largest term of the calculation. We consider verified the cancellation of the IR poles if, for any given number P of significant digits requested in the arbitrary precision evaluation framework, with $P > Q$, the sum of the coefficients yields 10^{-P+Q}, which is our explicit representation of zero. The results in Table 1 have been obtained with a precision request $P = 50$, while we observe a precision loss due to internal cancellations by $Q = 15$ orders of magnitude, eventually achieving control over 35 digits. The IR cancellation can be verified in greater detail by isolating subsets of contributions proportional to the same power of the electric charges of the initial state quark, final state lepton, and of the fermion running in the internal loops; each subset is separately IR finite.

Whenever possible, the precision losses can be reduced with a convenient choice of the MIs basis. In this computation we use the basis of Master Integrals automatically generated by the combined application of `Feynarts`, `ABISS` and `KIRA`, in order to test the efficiency of our code also with a suboptimal choice of Master Integrals. For more challenging calculations, as the full EW case, it is possible to improve such choice with the help of packages like for instance `Canonica` [117] or `LIBRA` [118]. The numerical control over the pole cancellation is the same as the one obtained using closed form expressions in terms of special functions for the Feynman integrals, given the possibility to push the
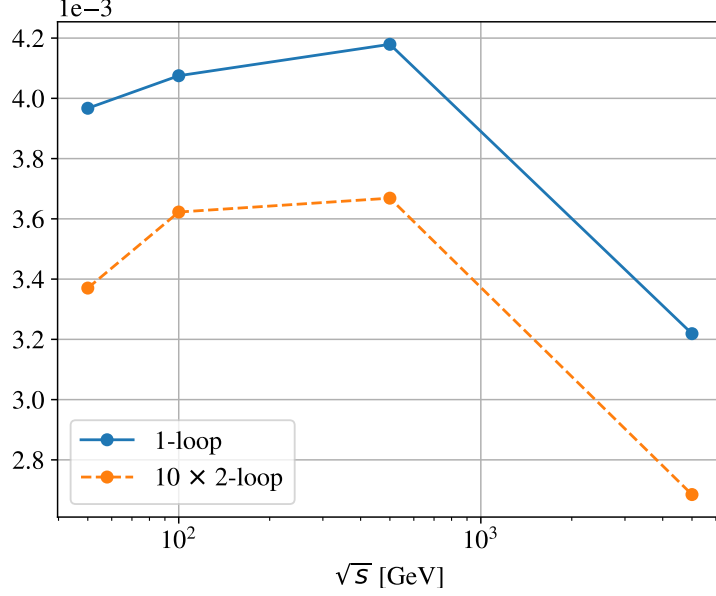
Figure 3. We plot the contribution to $\langle \mathcal{M} | \mathcal{M} \rangle$ coming from one- and two-loop diagrams for different values of $\sqrt{s}$ and $t = -s/4$. In particular, in solid blue we present $(4\pi\alpha_{\overline{\text{MS}}}^3) \, 2\text{Re}\langle \mathcal{M}^{(0,0)} | \mathcal{M}^{(0,1),fin} \rangle$, while in dashed orange $\alpha_{\overline{\text{MS}}}^4 \, 2\text{Re}\langle \mathcal{M}^{(0,0)} | \mathcal{M}^{(0,2),fin} \rangle$, with $\alpha_{\overline{\text{MS}}} = 1/128$. The two-loop contributions have been multiplied by a factor 10 to improve the readability.

precision to an arbitrary level. The solution of the MIs with a series expansion approach offers on the other hand a significant advantage for all those cases where a closed form solution is not viable: IR-finite integrals with several internal massive lines, but also IR-divergent integrals with 2 or 3 internal massive lines, which require a non trivial dedicated effort to be expressed in closed form [80].

In Table 1 we present also the result for the finite part of the interference term, which is in perfect agreement with the values presented in [97]. In Figure 3, we present additional values for the finite part of the interference term, calculated for different values of $\sqrt{s}$, whose behaviour displays the non trivial interplay of the different powers of Sudakov logarithms present in the virtual corrections.

4.3   Impact of a change of scheme

The results discussed in Section 3 are computed in terms of the $\overline{MS}$-renormalised electric charge $\alpha_{\overline{MS}}(\mu_R)$. The UV renormalised and IR subtracted squared amplitude, including the corrections up to second order, reads:

$$
\begin{aligned}
\langle \mathcal{M} | \mathcal{M} \rangle &= 16\pi^2 \alpha_{\overline{MS}}^2(\mu_R) \langle \mathcal{M}^{(0,0)} | \mathcal{M}^{(0,0)} \rangle \\
&\quad + 4\pi\alpha_{\overline{MS}}^3(\mu_R) \left[2\text{Re}\left(\langle \mathcal{M}^{(0,0)} | \mathcal{M}^{(0,1),fin} \rangle \right) \right] \\
&\quad + \alpha_{\overline{MS}}^4(\mu_R) \left[2\text{Re}\left(\langle \mathcal{M}^{(0,0)} | \mathcal{M}^{(0,2),fin} \rangle \right) + \langle \mathcal{M}^{(0,1),fin} | \mathcal{M}^{(0,1),fin} \rangle \right] + \cdots \\
&= \alpha_{\overline{MS}}^2(\mu_R) \, \bar{\mathcal{A}}_{00} + \alpha_{\overline{MS}}^3(\mu_R) \, \bar{\mathcal{A}}_{01} + \alpha_{\overline{MS}}^4(\mu_R) \left[\bar{\mathcal{A}}_{02} + \bar{\mathcal{A}}_{11} \right] + \cdots ,
\end{aligned}
\tag{4.2}
$$

Highest order	$\alpha(0)$ scheme	$\alpha_{\overline{MS}}(m_Z)$ scheme	Δ (%)
tree-level	46.742	53.546	12.707
one-loop	86.610	94.297	8.152
two-loop	97.158	97.919	0.777

Table 2. Numerical results of the squared virtual amplitude at $\mathcal{O}\left(\alpha^2\right)$, $\mathcal{O}\left(\alpha^3\right)$ and $\mathcal{O}\left(\alpha^4\right)$ in the two schemes for the renormalised electric charge, with $\alpha_{\overline{MS}}(m_Z) = 1/128$ and $\alpha(0) = 1/137$, in units of 10^{-4}. The last column shows the percentage difference $\Delta = 100 \, |\langle\mathcal{M}|\mathcal{M}\rangle_0 \, / \, \langle\mathcal{M}|\mathcal{M}\rangle_{\overline{MS}} - 1|$.

where the amplitudes $|\mathcal{M}^{(0,1),fin}\rangle$, $|\mathcal{M}^{(0,2),fin}\rangle$ and the abbreviations $\bar{\mathcal{A}}_{ij}$ depend on the renormalisation scale μ_R. Another choice to express the renormalised coupling is given by the on-shell scheme definition, at zero momentum transfer, $\alpha(0)$, from the study of the Thomson scattering. This second alternative provides an accurate description of the real-photon emission spectra, and it is thus of high phenomenological relevance. It is interesting to re-express Equation (4.2) in terms of the fine structure constant $\alpha(0)$, via a finite renormalisation. The relation between the on-shell and $\overline{MS}$ renormalised electric charges is given by [109]:

$$\alpha_{\overline{MS}}(\mu_R) \;=\; \frac{\alpha(0)}{1 - \Delta\alpha_{\overline{MS}}(\mu_R^2)} \;. \tag{4.3}$$

The definitions of the coefficients $\Delta\alpha_{\overline{MS}}^{(i)}(\mu_R^2)$ are reported in Appendix B, with the first order containing the hadronic part $\Delta\alpha_{\mathrm{had}}(\mu_R^2)$, necessary to express the light-quarks contribution. This quantity is extracted from the experimental data of the cross section $e^+e^- \to$ hadrons and, in the case of $\mu_R = m_Z$, it is possible to use the determination from [119]: $\Delta\alpha_{\mathrm{had}}(m_Z^2) = 0.027572 \pm 0.000359$. In the following we perform a technical comparison to test the perturbative convergence of the results when increasing the order of the perturbative approximation. Expanding Equation (4.3) one gets:

$$\alpha_{\overline{MS}}(m_Z) \;=\; \alpha(0) \left[1 + \alpha(0)\Delta\alpha_{\overline{MS}}^{(1)}(m_Z^2) + \alpha(0)^2 \left(\left(\Delta\alpha_{\overline{MS}}^{(1)}(m_Z^2)\right)^2 + \Delta\alpha_{\overline{MS}}^{(2)}(m_Z^2) \right) \right] \;. \tag{4.4}$$

Replacing the couplings in Equation (4.2) with Equation (4.4), we obtain:

$$\begin{aligned}
\langle\mathcal{M}|\mathcal{M}\rangle = \alpha(0)^2\,\bar{\mathcal{A}}_{00} \;+\;& \alpha(0)^3 \left[\bar{\mathcal{A}}_{01} + 2\Delta\alpha_{\overline{MS}}^{(1)}(m_Z^2)\,\bar{\mathcal{A}}_{00} \right] \\
+\,& \alpha(0)^4 \left[\bar{\mathcal{A}}_{02} + \bar{\mathcal{A}}_{11} + 3\Delta\alpha_{\overline{MS}}^{(1)}(m_Z^2)\,\bar{\mathcal{A}}_{01} \right. \\
&\left. +\, 2\Delta\alpha_{\overline{MS}}^{(2)}(m_Z^2)\,\bar{\mathcal{A}}_{00} + 3\left(\Delta\alpha_{\overline{MS}}^{(1)}(m_Z^2)\right)^2 \bar{\mathcal{A}}_{00} \right] \;+\; \cdots
\end{aligned} \tag{4.5}$$

In Table 2 we compare the sum of the contributions to the squared matrix element, using as renormalised electric charge $\alpha_{\overline{MS}}(m_Z)$ or $\alpha(0)$[6]. We consider different approximations: tree-level only, tree-level and one-loop corrections, the sum of tree-level, one-loop and of the

---

[6]Note that in order to use the formulae in [109], we have to account for the different normalisation of the Feynman integrals by a factor S_ϵ.

two-loop $\langle \mathcal{M}^{(0,0)} | \mathcal{M}^{(0,2),fin} \rangle$ term. At tree level the difference between the results is purely due to the ratio of the coupling constants $\left(\alpha_{\overline{MS}}(m_Z)/\alpha(0) \right)^2$. In the one-loop virtual corrections there are two subsets: the self-energy corrections together with the electric charge counterterms and the group composed by vertex and box corrections. The former, combined with the tree level, features in the two schemes much closer results compared to the tree-level case. The latter on the other hand are still evaluated with tree level couplings and, given the large difference between the couplings in the two schemes, they yield a difference between the results at the 8% level. It is thus interesting to observe the impact of the two-loop corrections, which include the renormalisation of the couplings present in the one-loop diagrams. Thanks to this additional step, also the one-loop vertices and boxes are evaluated with effective couplings closer in value, reducing the distance between the two schemes at sub percent level.

5   Conclusions

We have presented in this paper the evaluation in QED of the two-loop virtual corrections to the process of production of a massive lepton-pair, in quark-antiquark annihilation. These results illustrate a general systematic approach to the evaluation of the complete two-loop EW corrections to the scattering processes relevant for the precision physics program at the LHC. The tools needed to accomplish this ambitious task are coherently organized in the OCEANN framework. One of the major technical issues, the evaluation of the Feynman integrals, is solved with a solution by series expansions, which provides results with arbitrary precision and a complete control over the cancellation of the UV and IR divergences. The validation of these QED results with the literature supports the robustness of the approach, in a stress case from the point of view of the numerical cancellations and of potential precision losses.

A Renormalisation relations

We report here the basic definitions that we have followed for the semi-analytical computation of the counterterms, needed to obtain the complete two-loop renormalised amplitude.

A.1 Electric charge renormalisation within the $\overline{MS}$ scheme

The renormalisation of the electric charge has been carried out following the same scheme for both the diagrammatic contributions and the subtraction operators. The relation between the bare electric charge and the renormalised one is defined up to the second order in α by introducing the counterterms

$$e_0 = e + \delta e = e\, Z_e = e\left(1 + \delta Z_e^{(1)} + \delta Z_e^{(2)} + \mathcal{O}(\alpha^3)\right) . \tag{A.1}$$

Following the on-shell renormalisation scheme, the Ward Identity associated to the residual $U(1)_{em}$ gauge invariance ensures that the renormalisation of the electric charge follows entirely from the transverse photon-photon self-energy $\Sigma_T^{AA}(q^2)$[103, 105, 109], via the renormalisation condition on the $\gamma f f$ vertex that relates Z_e with the photon wavefunction counterterm $Z_{AA} = 1 + \delta Z_{AA}^{OS} = 1 + \delta Z_{AA}^{OS(1)} + \delta Z_{AA}^{OS(2)} + \cdots$:

$$Z_e^{OS} = \frac{1}{\sqrt{Z_{AA}^{OS}}} = \frac{1}{\sqrt{1 + \delta Z_{AA}^{OS(1)} + \delta Z_{AA}^{OS(2)} + \ldots}} , \tag{A.2}$$

with

$$\delta Z_{AA}^{OS} = -\left.\frac{\partial \Sigma_T^{AA}(q^2)}{\partial q^2}\right|_{q^2=0} . \tag{A.3}$$

In the $\overline{MS}$ scheme, only the divergent terms of the self-energies are kept in the definitions of the counterterms, and an additional dependence on the renormalisation scale μ_R and on the regularisation 't Hooft scale μ is introduced together with an overall factor $S_\epsilon = (4\pi e^{-\gamma_E})^\epsilon$:

$$\delta Z_e^{\overline{MS}(1)} = S_\epsilon \left(\frac{\mu^2}{\mu_R^2}\right)^\epsilon \left[-\frac{1}{2}\delta Z_{AA}^{OS(1)}\big|_{\text{poles}}\right] , \tag{A.4}$$

$$\delta Z_e^{\overline{MS}(2)} = S_\epsilon^2 \left(\frac{\mu^2}{\mu_R^2}\right)^{2\epsilon} \left[-\frac{1}{2}\delta Z_{AA}^{OS(2)}\big|_{\text{poles}} + \frac{3}{8}\left(\delta Z_{AA}^{OS(1)}\big|_{\text{poles}}\right)^2\right] .$$

We have checked our results to be in agreement with an arbitrary number of digits with the expressions provided in [97], that we that we report here for completeness after switching to our notation:

$$\delta Z_e^{\overline{MS}(1)} = \frac{\alpha(\mu_R)}{4\pi} S_\epsilon \left(\frac{\mu^2}{\mu_R^2}\right)^\epsilon \left[\frac{2}{3\epsilon}\sum_k N_k Q_k^2\right] , \tag{A.5}$$

$$\delta Z_e^{\overline{MS}(2)} = \left(\frac{\alpha(\mu_R)}{4\pi}\right)^2 S_\epsilon^2 \left(\frac{\mu^2}{\mu_R^2}\right)^{2\epsilon} \left[\frac{2}{3\epsilon^2}\left(\sum_k N_k Q_k^2\right)^2 + \frac{1}{\epsilon}\sum_k N_k Q_k^4\right] .$$

In our computation, both the UV renormalisation procedure and the IR subtraction of divergences have been realized fixing for convenience $\mu = \mu_R$, resulting in an expression for δZ_e completely independent of any arbitrary scale.

A.2 Fermion mass and wave-function on-shell renormalisation

The fermion fields and masses are renormalised up to $\mathcal{O}(\alpha^2)$ with the wave-function renormalisation constants:

$$m_{f0} = m_f + \delta m_f = m_f + \delta m_f^{(1)} + \mathcal{O}(\alpha^2) , \tag{A.6}$$

$$f_0 = (Z_f)^{\frac{1}{2}} f = \left[1 + \frac{1}{2}\delta Z_f^{(1)} + \frac{1}{2}\delta Z_f^{(2)} - \frac{1}{8}\left(\delta Z_f^{(1)}\right)^2 + \mathcal{O}(\alpha^3) \right] f .$$

The counterterm expressions has been computed with a semi-analytical evaluation fixing the on-shell renormalisation conditions satisfied from the fermion two-point vertex function. Following the same notation of [103, 104] with $\Sigma_L^{f\bar{f}} = \Sigma_R^{f\bar{f}} = \Sigma^{f\bar{f}}$, we have:

$$\delta m_f^{(1)} = m_f \left[\Sigma^{f\bar{f}(1)}(m_f^2) + \Sigma_S^{f\bar{f}(1)}(m_f{}^2) \right] , \tag{A.7}$$

$$\delta Z_f^{(1)} = -\Sigma^{f\bar{f}(1)}(m_f^2) - 2m_f^2 \frac{\partial}{\partial p^2}\left[\Sigma^{f\bar{f}(1)}(p^2) + \Sigma_S^{f\bar{f}(1)}(p^2) \right]\Big|_{p^2=m_f^2} ,$$

$$\delta Z_f^{(2)} = -\Sigma^{f\bar{f}(2)}(m_f^2) - 2m_f^2 \frac{\partial}{\partial p^2}\left[\Sigma^{f\bar{f}(2)}(p^2) + \Sigma_S^{f\bar{f}(2)}(p^2) \right]\Big|_{p^2=m_f^2} .$$

Our results for the fermion counterterms are in agreement with the analytic formula present in [97] after including the self-energy dependence on the different internal masses.

B Photon vacuum polarization

The change of renormalisation scheme for the QED coupling can be expressed with a finite renormalisation between the on-shell one and $\overline{MS}$ schemes. Following the approach described in [109], we define the photon vacuum polarization function from the self-energy expression:

$$\Sigma_T^{AA}(q^2) = -(4\pi\alpha)\, q^2 \Pi_{\gamma\gamma}(q^2) . \tag{B.1}$$

Indicating with $\bar{\Pi}^{(i)}(0)$ only the ϵ-divergent contribution of $\Pi^{(i)}(0)$ we therefore link the photon vacuum polarization function with our definitions of wave-function counterterms:

$$\delta Z_{AA}^{OS} = 4\pi\alpha\, \Pi_{\gamma\gamma}(0) \implies \delta Z_{AA}^{OS(i)} = 4\pi\alpha^i\, \Pi_{\gamma\gamma}^{(i)}(0) , \tag{B.2}$$

$$\delta Z_{AA}^{\overline{MS}} = 4\pi\alpha_{\overline{MS}}\, \bar{\Pi}_{\gamma\gamma}(0) \implies \delta Z_{AA}^{\overline{MS}(i)} = 4\pi(\alpha_{\overline{MS}})^i\, S_\epsilon^i\, \bar{\Pi}_{\gamma\gamma}^{(i)}(0) .$$

The two expressions are related by the definition of the bare coupling

$$\alpha_0 = \alpha Z_e^2 = \alpha\left(Z_{AA}^{OS}\right)^{-1} = \alpha_{\overline{MS}}\left(Z_{AA}^{\overline{MS}}\right)^{-1} , \tag{B.3}$$

that we can expand up to the second order in α and/or $\alpha_{\overline{MS}}$ (since $\mathcal{O}(\alpha) = \mathcal{O}(\alpha_{\overline{MS}})$):

$$\alpha_{\overline{MS}} = \alpha - 4\pi\alpha\alpha_{\overline{MS}}\left(\Pi_{\gamma\gamma}^{(1)}(0) - \bar{\Pi}_{\gamma\gamma}^{(1)}(0)\right) \tag{B.4}$$

$$- 4\pi\alpha(\alpha_{\overline{MS}})^2\left(\frac{\alpha}{\alpha_{\overline{MS}}}\Pi_{\gamma\gamma}^{(2)}(0) - \bar{\Pi}_{\gamma\gamma}^{(2)}(0)\right) + \mathcal{O}(\alpha^4)$$

$$= \alpha \left(1 - 4\pi\alpha_{\overline{MS}}\hat{\Pi}^{(1)}_{\gamma\gamma}(0) - 4\pi(\alpha_{\overline{MS}})^2 \hat{\Pi}^{(2)}_{\gamma\gamma}(0) + \mathcal{O}(\alpha^3) \right) ,$$

where the factors S^i_ϵ have been removed by rescaling the t'Hooft parameter in $\Pi_{\gamma\gamma}(0)$ with $\mu \to \sqrt{e^{\gamma_E}/4\pi}\, \mu$. In the last row we exploited the fact that $\alpha/\alpha_{\overline{MS}} = 1 + O(\alpha)$ and we defined $\hat{\Pi}^{(i)}_{\gamma\gamma}(0)$ as the finite remainder from the difference $\Pi^{(i)}_{\gamma\gamma}(0) - \bar{\Pi}^{(i)}_{\gamma\gamma}(0)$. Equation B.4 directly leads to the definition of $\Delta\alpha_{\overline{MS}}(m_Z^2)$ after setting $\mu_R = m_Z$. The photon vacuum polarisation can be decomposed as:

$$\Pi_{\gamma\gamma}(0) = \Pi^{(\text{lep})}_{\gamma\gamma}(0) + \Pi^{(\text{top})}_{\gamma\gamma}(0) + \Pi^{(5)}_{\gamma\gamma}(0) \tag{B.5}$$
$$= \Pi^{(\text{lep})}_{\gamma\gamma}(0) + \Pi^{(\text{top})}_{\gamma\gamma}(0) + \text{Re}(\Pi^{(5)}_{\gamma\gamma}(m_Z^2)) - \frac{\Delta\alpha_{\text{had}}(m_Z^2)}{4\pi\alpha} ,$$

where (lep) and (top) are the perturbative contributions from the leptons and the massive top quarks, (5) is the contribution from the five light quarks and $\Delta\alpha_{\text{had}}(m_Z^2) = 4\pi\alpha \left(\text{Re}(\Pi^{(5)}_{\gamma\gamma}(m_Z^2)) - \Pi^{(5)}_{\gamma\gamma}(0) \right)$ is derived via a dispersion relation from the experimental cross section of $e^+e^- \to$ hadrons. In conclusion we obtain:

$$\Delta\alpha_{\overline{MS}}(m_Z^2) = \Delta\alpha^{(1)}_{\overline{MS}}(m_Z^2) + \Delta\alpha^{(2)}_{\overline{MS}}(m_Z^2) + \mathcal{O}(\alpha^3) = \tag{B.6}$$
$$= -4\pi\alpha_{\overline{MS}} \left[\hat{\Pi}^{(\text{lep})(1)}_{\gamma\gamma}(0) + \hat{\Pi}^{(\text{top})(1)}_{\gamma\gamma}(0) + \text{Re}(\hat{\Pi}^{(5)(1)}_{\gamma\gamma}(m_Z^2)) - \frac{\Delta\alpha_{\text{had}}(m_Z^2)}{4\pi\alpha} \right]$$
$$- 4\pi(\alpha_{\overline{MS}})^2 \left[\hat{\Pi}^{(\text{lep})(2)}_{\gamma\gamma}(0) + \hat{\Pi}^{(\text{top})(2)}_{\gamma\gamma}(0) + \text{Re}(\hat{\Pi}^{(5)(2)}_{\gamma\gamma}(m_Z^2)) \right] + \mathcal{O}(\alpha^3) .$$

The term $\Delta\alpha_{\text{had}}(m_Z^2)$ starts at $\mathcal{O}(\alpha)$ and takes part to the definition of $\Delta\alpha^{(1)}_{\overline{MS}}(m_Z^2)$, thus affecting the change of scheme for the virtual amplitude starting from NLO.

References

[1] S. Drell and T.-M. Yan, *Massive Lepton Pair Production in Hadron-Hadron Collisions at High-Energies*, *Phys. Rev. Lett.* **25** (1970) 316–320.

[2] CDF, D0 collaboration, T. E. W. Group, *2012 Update of the Combination of CDF and D0 Results for the Mass of the W Boson*, 1204.0042.

[3] ATLAS collaboration, M. Aaboud et al., *Measurement of the W-boson mass in pp collisions at $\sqrt{s} = 7$ TeV with the ATLAS detector*, *Eur. Phys. J. C* **78** (2018) 110, [1701.07240].

[4] CDF, D0 collaboration, T. A. Aaltonen et al., *Tevatron Run II combination of the effective leptonic electroweak mixing angle*, *Phys. Rev. D* **97** (2018) 112007, [1801.06283].

[5] ATLAS collaboration, *Measurement of the effective leptonic weak mixing angle using electron and muon pairs from Z-boson decay in the ATLAS experiment at $\sqrt{s} = 8$ TeV*, *ATLAS-CONF-2018-037* (7, 2018) .

[6] CMS collaboration, *Measurement of the Drell-Yan forward-backward asymmetry and of the effective leptonic weak mixing angle using proton-proton collisions at 13 TeV*, tech. rep., CERN, Geneva, 2024.

[7] C. M. Carloni Calame, M. Chiesa, H. Martinez, G. Montagna, O. Nicrosini, F. Piccinini and A. Vicini, *Precision Measurement of the W-Boson Mass: Theoretical Contributions and Uncertainties*, *Phys. Rev. D* **96** (2017) 093005, [1612.02841].

[8] M. Chiesa, F. Piccinini and A. Vicini, *Direct determination of* $\sin^2 \theta_{eff}^\ell$ *at hadron colliders*, *Phys. Rev. D* **100** (2019) 071302, [1906.11569].

[9] E. Bagnaschi and A. Vicini, *Parton Density Uncertainties and the Determination of Electroweak Parameters at Hadron Colliders*, *Phys. Rev. Lett.* **126** (2021) 041801, [1910.04726].

[10] A. Behring, F. Buccioni, F. Caola, M. Delto, M. Jaquier, K. Melnikov and R. Röntsch, *Estimating the impact of mixed QCD-electroweak corrections on the W-mass determination at the LHC*, *Phys. Rev. D* **103** (2021) 113002, [2103.02671].

[11] L. Rottoli, P. Torrielli and A. Vicini, *Determination of the W-boson mass at hadron colliders*, *Eur. Phys. J. C* **83** (2023) 948, [2301.04059].

[12] P. Torrielli, L. Rottoli and A. Vicini, *A new observable for W-mass determination*, *PoS* **RADCOR2023** (2024) 038, [2308.15993].

[13] C. Duhr, F. Dulat and B. Mistlberger, *Drell-Yan Cross Section to Third Order in the Strong Coupling Constant*, *Phys. Rev. Lett.* **125** (2020) 172001, [2001.07717].

[14] C. Duhr, F. Dulat and B. Mistlberger, *Charged current Drell-Yan production at* N^3LO, *JHEP* **11** (2020) 143, [2007.13313].

[15] C. Duhr and B. Mistlberger, *Lepton-pair production at hadron colliders at* N^3LO *in QCD*, *JHEP* **03** (2022) 116, [2111.10379].

[16] S. Dittmaier and M. Krämer, *Electroweak radiative corrections to W boson production at hadron colliders*, *Phys. Rev. D* **65** (2002) 073007, [hep-ph/0109062].

[17] U. Baur and D. Wackeroth, *Electroweak radiative corrections to* $p\bar{p} \to W^\pm \to \ell^\pm \nu$ *beyond the pole approximation*, *Phys. Rev. D* **70** (2004) 073015, [hep-ph/0405191].

[18] V. Zykunov, *Radiative corrections to the Drell-Yan process at large dilepton invariant masses*, *Phys. Atom. Nucl.* **69** (2006) 1522.

[19] A. Arbuzov, D. Bardin, S. Bondarenko, P. Christova, L. Kalinovskaya, G. Nanava and R. Sadykov, *One-loop corrections to the Drell-Yan process in SANC. I. The Charged current case*, *Eur. Phys. J. C* **46** (2006) 407–412, [hep-ph/0506110].

[20] C. Carloni Calame, G. Montagna, O. Nicrosini and A. Vicini, *Precision electroweak calculation of the charged current Drell-Yan process*, *JHEP* **12** (2006) 016, [hep-ph/0609170].

[21] U. Baur, O. Brein, W. Hollik, C. Schappacher and D. Wackeroth, *Electroweak radiative corrections to neutral current Drell-Yan processes at hadron colliders*, *Phys. Rev. D* **65** (2002) 033007, [hep-ph/0108274].

[22] V. Zykunov, *Weak radiative corrections to Drell-Yan process for large invariant mass of di-lepton pair*, *Phys. Rev. D* **75** (2007) 073019, [hep-ph/0509315].

[23] C. Carloni Calame, G. Montagna, O. Nicrosini and A. Vicini, *Precision electroweak calculation of the production of a high transverse-momentum lepton pair at hadron colliders*, *JHEP* **10** (2007) 109, [0710.1722].

[24] A. Arbuzov, D. Bardin, S. Bondarenko, P. Christova, L. Kalinovskaya, G. Nanava and R. Sadykov, *One-loop corrections to the Drell–Yan process in SANC. (II). The Neutral current case*, *Eur. Phys. J. C* **54** (2008) 451–460, [0711.0625].

[25] S. Dittmaier and M. Huber, *Radiative corrections to the neutral-current Drell-Yan process in the Standard Model and its minimal supersymmetric extension*, *JHEP* **01** (2010) 060, [`0911.2329`].

[26] R. Bonciani, L. Buonocore, M. Grazzini, S. Kallweit, N. Rana, F. Tramontano and A. Vicini, *Mixed Strong-Electroweak Corrections to the Drell-Yan Process*, *Phys. Rev. Lett.* **128** (2022) 012002, [`2106.11953`].

[27] F. Buccioni, F. Caola, H. A. Chawdhry, F. Devoto, M. Heller, A. von Manteuffel, K. Melnikov, R. Röntsch and C. Signorile-Signorile, *Mixed QCD-electroweak corrections to dilepton production at the LHC in the high invariant mass region*, *JHEP* **06** (2022) 022, [`2203.11237`].

[28] T. Armadillo, R. Bonciani, S. Devoto, N. Rana and A. Vicini, *Two-loop mixed QCD-EW corrections to charged current Drell-Yan*, *JHEP* **07** (2024) 265, [`2405.00612`].

[29] B. Jantzen, J. H. Kuhn, A. A. Penin and V. A. Smirnov, *Two-loop electroweak logarithms in four-fermion processes at high energy*, *Nucl. Phys. B* **731** (2005) 188–212, [`hep-ph/0509157`].

[30] A. Denner, B. Jantzen and S. Pozzorini, *Two-loop electroweak next-to-leading logarithmic corrections to massless fermionic processes*, *Nucl. Phys. B* **761** (2007) 1–62, [`hep-ph/0608326`].

[31] M. Chiesa, C. L. Del Pio and F. Piccinini, *On electroweak corrections to neutral current Drell-Yan with the POWHEG BOX*, `2402.14659`.

[32] G. Altarelli, R. Ellis and G. Martinelli, *Large Perturbative Corrections to the Drell-Yan Process in QCD*, *Nucl. Phys. B* **157** (1979) 461–497.

[33] R. Hamberg, W. van Neerven and T. Matsuura, *A complete calculation of the order α_s^2 correction to the Drell-Yan K factor*, *Nucl. Phys. B* **359** (1991) 343–405.

[34] R. V. Harlander and W. B. Kilgore, *Next-to-next-to-leading order Higgs production at hadron colliders*, *Phys. Rev. Lett.* **88** (2002) 201801, [`hep-ph/0201206`].

[35] C. Anastasiou, L. J. Dixon, K. Melnikov and F. Petriello, *Dilepton rapidity distribution in the Drell-Yan process at NNLO in QCD*, *Phys. Rev. Lett.* **91** (2003) 182002, [`hep-ph/0306192`].

[36] C. Anastasiou, L. J. Dixon, K. Melnikov and F. Petriello, *High precision QCD at hadron colliders: Electroweak gauge boson rapidity distributions at NNLO*, *Phys. Rev. D* **69** (2004) 094008, [`hep-ph/0312266`].

[37] K. Melnikov and F. Petriello, *Electroweak gauge boson production at hadron colliders through $\mathcal{O}(\alpha_s^2)$*, *Phys. Rev. D* **74** (2006) 114017, [`hep-ph/0609070`].

[38] S. Catani, L. Cieri, G. Ferrera, D. de Florian and M. Grazzini, *Vector boson production at hadron colliders: a fully exclusive QCD calculation at NNLO*, *Phys. Rev. Lett.* **103** (2009) 082001, [`0903.2120`].

[39] S. Catani, G. Ferrera and M. Grazzini, *W Boson Production at Hadron Colliders: The Lepton Charge Asymmetry in NNLO QCD*, *JHEP* **05** (2010) 006, [`1002.3115`].

[40] S. Camarda, L. Cieri and G. Ferrera, *Drell–Yan lepton-pair production: qT resummation at N3LL accuracy and fiducial cross sections at N3LO*, *Phys. Rev. D* **104** (2021) L111503, [`2103.04974`].

[41] X. Chen, T. Gehrmann, E. W. N. Glover, A. Huss, P. F. Monni, E. Re, L. Rottoli and P. Torrielli, *Third-Order Fiducial Predictions for Drell-Yan Production at the LHC*, *Phys. Rev. Lett.* **128** (2022) 252001, [2203.01565].

[42] T. Neumann and J. Campbell, *Fiducial Drell-Yan production at the LHC improved by transverse-momentum resummation at N4LLp+N3LO*, *Phys. Rev. D* **107** (2023) L011506, [2207.07056].

[43] J. Campbell and T. Neumann, *Third order QCD predictions for fiducial W-boson production*, *JHEP* **11** (2023) 127, [2308.15382].

[44] X. Chen, T. Gehrmann, N. Glover, A. Huss, T.-Z. Yang and H. X. Zhu, *Dilepton Rapidity Distribution in Drell-Yan Production to Third Order in QCD*, *Phys. Rev. Lett.* **128** (2022) 052001, [2107.09085].

[45] X. Chen, T. Gehrmann, N. Glover, A. Huss, T.-Z. Yang and H. X. Zhu, *Transverse mass distribution and charge asymmetry in W boson production to third order in QCD*, *Phys. Lett. B* **840** (2023) 137876, [2205.11426].

[46] S. Moch and A. Vogt, *Higher-order soft corrections to lepton pair and Higgs boson production*, *Phys. Lett. B* **631** (2005) 48–57, [hep-ph/0508265].

[47] E. Laenen and L. Magnea, *Threshold resummation for electroweak annihilation from DIS data*, *Phys. Lett. B* **632** (2006) 270–276, [hep-ph/0508284].

[48] V. Ravindran, *On Sudakov and soft resummations in QCD*, *Nucl. Phys. B* **746** (2006) 58–76, [hep-ph/0512249].

[49] V. Ravindran, *Higher-order threshold effects to inclusive processes in QCD*, *Nucl. Phys. B* **752** (2006) 173–196, [hep-ph/0603041].

[50] D. de Florian and J. Mazzitelli, *A next-to-next-to-leading order calculation of soft-virtual cross sections*, *JHEP* **12** (2012) 088, [1209.0673].

[51] T. Ahmed, M. Mahakhud, N. Rana and V. Ravindran, *Drell-Yan Production at Threshold to Third Order in QCD*, *Phys. Rev. Lett.* **113** (2014) 112002, [1404.0366].

[52] S. Catani, L. Cieri, D. de Florian, G. Ferrera and M. Grazzini, *Threshold resummation at N^3LL accuracy and soft-virtual cross sections at N^3LO*, *Nucl. Phys. B* **888** (2014) 75–91, [1405.4827].

[53] Y. Li, A. von Manteuffel, R. M. Schabinger and H. X. Zhu, *Soft-virtual corrections to Higgs production at N^3LO*, *Phys. Rev. D* **91** (2015) 036008, [1412.2771].

[54] A. H. Ajjath, P. Mukherjee and V. Ravindran, *On next to soft corrections to Drell-Yan and Higgs Boson productions*, 2006.06726.

[55] G. 't Hooft and M. J. G. Veltman, *Scalar One Loop Integrals*, *Nucl. Phys. B* **153** (1979) 365–401.

[56] F. Buccioni, J.-N. Lang, J. M. Lindert, P. Maierhöfer, S. Pozzorini, H. Zhang and M. F. Zoller, *OpenLoops 2*, *Eur. Phys. J. C* **79** (2019) 866, [1907.13071].

[57] S. Actis, A. Denner, L. Hofer, J.-N. Lang, A. Scharf and S. Uccirati, *RECOLA: REcursive Computation of One-Loop Amplitudes*, *Comput. Phys. Commun.* **214** (2017) 140–173, [1605.01090].

[58] A. Denner, J.-N. Lang and S. Uccirati, *Recola2: REcursive Computation of One-Loop Amplitudes 2*, *Comput. Phys. Commun.* **224** (2018) 346–361, [1711.07388].

[59] G. Balossini, G. Montagna, C. M. Carloni Calame, M. Moretti, M. Treccani, O. Nicrosini, F. Piccinini and A. Vicini, *Electroweak & QCD corrections to Drell Yan processes*, *Acta Phys. Polon. B* **39** (2008) 1675, [0805.1129].

[60] G. Balossini, G. Montagna, C. M. Carloni Calame, M. Moretti, O. Nicrosini, F. Piccinini, M. Treccani and A. Vicini, *Combination of electroweak and QCD corrections to single W production at the Fermilab Tevatron and the CERN LHC*, *JHEP* **01** (2010) 013, [0907.0276].

[61] C. Bernaciak and D. Wackeroth, *Combining NLO QCD and Electroweak Radiative Corrections to W boson Production at Hadron Colliders in the POWHEG Framework*, *Phys. Rev. D* **85** (2012) 093003, [1201.4804].

[62] L. Barze, G. Montagna, P. Nason, O. Nicrosini and F. Piccinini, *Implementation of electroweak corrections in the POWHEG BOX: single W production*, *JHEP* **04** (2012) 037, [1202.0465].

[63] L. Barze, G. Montagna, P. Nason, O. Nicrosini, F. Piccinini and A. Vicini, *Neutral current Drell-Yan with combined QCD and electroweak corrections in the POWHEG BOX*, *Eur. Phys. J. C* **73** (2013) 2474, [1302.4606].

[64] R. Frederix, S. Frixione, V. Hirschi, D. Pagani, H. S. Shao and M. Zaro, *The automation of next-to-leading order electroweak calculations*, *JHEP* **07** (2018) 185, [1804.10017].

[65] M. Delto, M. Jaquier, K. Melnikov and R. Röntsch, *Mixed QCD⊗QED corrections to on-shell Z boson production at the LHC*, *JHEP* **01** (2020) 043, [1909.08428].

[66] L. Cieri, D. de Florian, M. Der and J. Mazzitelli, *Mixed QCD⊗QED corrections to exclusive Drell Yan production using the q_T -subtraction method*, *JHEP* **09** (2020) 155, [2005.01315].

[67] R. Bonciani, F. Buccioni, R. Mondini and A. Vicini, *Double-real corrections at $\mathcal{O}(\alpha\alpha_s)$ to single gauge boson production*, *Eur. Phys. J. C* **77** (2017) 187, [1611.00645].

[68] R. Bonciani, F. Buccioni, N. Rana, I. Triscari and A. Vicini, *NNLO QCD×EW corrections to Z production in the $q\bar{q}$ channel*, *Phys. Rev. D* **101** (2020) 031301, [1911.06200].

[69] R. Bonciani, F. Buccioni, N. Rana and A. Vicini, *NNLO QCD×EW corrections to on-shell Z production*, *Phys. Rev. Lett.* **125** (2020) 232004, [2007.06518].

[70] R. Bonciani, F. Buccioni, N. Rana and A. Vicini, *On-shell Z boson production at hadron colliders through $\mathcal{O}(\alpha\alpha_s)$*, *JHEP* **02** (2022) 095, [2111.12694].

[71] F. Buccioni, F. Caola, M. Delto, M. Jaquier, K. Melnikov and R. Röntsch, *Mixed QCD-electroweak corrections to on-shell Z production at the LHC*, *Phys. Lett. B* **811** (2020) 135969, [2005.10221].

[72] A. Behring, F. Buccioni, F. Caola, M. Delto, M. Jaquier, K. Melnikov and R. Röntsch, *Mixed QCD-electroweak corrections to W-boson production in hadron collisions*, *Phys. Rev. D* **103** (2021) 013008, [2009.10386].

[73] S. Dittmaier, A. Huss and C. Schwinn, *Mixed QCD-electroweak $\mathcal{O}(\alpha_s\alpha)$ corrections to Drell-Yan processes in the resonance region: pole approximation and non-factorizable corrections*, *Nucl. Phys. B* **885** (2014) 318–372, [1403.3216].

[74] S. Dittmaier, A. Huss and C. Schwinn, *Dominant mixed QCD-electroweak $O(\alpha_s\alpha)$ corrections to Drell–Yan processes in the resonance region*, *Nucl. Phys. B* **904** (2016) 216–252, [1511.08016].

[75] S. Dittmaier, T. Schmidt and J. Schwarz, *Mixed NNLO QCD×electroweak corrections of* $\mathcal{O}(N_f\alpha_s\alpha)$ *to single-W/Z production at the LHC*, *JHEP* **12** (2020) 201, [2009.02229].

[76] S. Dittmaier, A. Huss and J. Schwarz, *Mixed NNLO QCD × electroweak corrections to single-Z production in pole approximation: differential distributions and forward-backward asymmetry*, 2401.15682.

[77] D. de Florian, M. Der and I. Fabre, *QCD⊕QED NNLO corrections to Drell Yan production*, *Phys. Rev. D* **98** (2018) 094008, [1805.12214].

[78] T. Armadillo, R. Bonciani, S. Devoto, N. Rana and A. Vicini, *Two-loop mixed QCD-EW corrections to neutral current Drell-Yan*, *JHEP* **05** (2022) 072, [2201.01754].

[79] M. Heller, A. von Manteuffel, R. M. Schabinger and H. Spiesberger, *Mixed EW-QCD two-loop amplitudes for* $q\bar{q} \to \ell^+\ell^-$ *and* γ_5 *scheme independence of multi-loop corrections*, *JHEP* **05** (2021) 213, [2012.05918].

[80] M. Heller, A. von Manteuffel and R. M. Schabinger, *Multiple polylogarithms with algebraic arguments and the two-loop EW-QCD Drell-Yan master integrals*, *Phys. Rev. D* **102** (2020) 016025, [1907.00491].

[81] S. M. Hasan and U. Schubert, *Master Integrals for the mixed QCD-QED corrections to the Drell-Yan production of a massive lepton pair*, *JHEP* **11** (2020) 107, [2004.14908].

[82] L. Buonocore, M. Grazzini, S. Kallweit, C. Savoini and F. Tramontano, *Mixed QCD-EW corrections to* $pp \to \ell\nu_\ell + X$ *at the LHC*, *Phys. Rev. D* **103** (2021) 114012, [2102.12539].

[83] F. Moriello, *Generalised power series expansions for the elliptic planar families of Higgs + jet production at two loops*, *JHEP* **01** (2020) 150, [1907.13234].

[84] M. Hidding, *DiffExp, a Mathematica package for computing Feynman integrals in terms of one-dimensional series expansions*, *Comput. Phys. Commun.* **269** (2021) 108125, [2006.05510].

[85] T. Armadillo, R. Bonciani, S. Devoto, N. Rana and A. Vicini, *Evaluation of Feynman integrals with arbitrary complex masses via series expansions*, *Comput. Phys. Commun.* **282** (2023) 108545, [2205.03345].

[86] X. Liu and Y.-Q. Ma, *AMFlow: A Mathematica package for Feynman integrals computation via auxiliary mass flow*, *Comput. Phys. Commun.* **283** (2023) 108565, [2201.11669].

[87] R. M. Prisco, J. Ronca and F. Tramontano, *LINE: Loop Integrals Numerical Evaluation*, *JHEP* **07** (2025) 219, [2501.01943].

[88] T. Armadillo, *Evaluating Feynman Integrals through differential equations and series expansions*, 2502.14742.

[89] N. Agarwal, L. Magnea, C. Signorile-Signorile and A. Tripathi, *The infrared structure of perturbative gauge theories*, *Phys. Rept.* **994** (2023) 1–120, [2112.07099].

[90] WORKING GROUP ON RADIATIVE CORRECTIONS, MONTE CARLO GENERATORS FOR LOW ENERGIES collaboration, S. Actis et al., *Quest for precision in hadronic cross sections at low energy: Monte Carlo tools vs. experimental data*, *Eur. Phys. J. C* **66** (2010) 585–686, [0912.0749].

[91] C. M. Carloni Calame, H. Czyz, J. Gluza, M. Gunia, G. Montagna, O. Nicrosini, F. Piccinini, T. Riemann and M. Worek, *NNLO massive corrections to Bhabha scattering*

and theoretical precision of BabaYaga@NLO, *Nucl. Phys. B Proc. Suppl.* **225-227** (2012) 293–297, [`1112.2851`].

[92] C. Carloni Calame, H. Czyz, J. Gluza, M. Gunia, G. Montagna, O. Nicrosini, F. Piccinini, T. Riemann and M. Worek, *NNLO leptonic and hadronic corrections to Bhabha scattering and luminosity monitoring at meson factories*, *JHEP* **07** (2011) 126, [`1106.3178`].

[93] P. Banerjee, T. Engel, A. Signer and Y. Ulrich, *QED at NNLO with McMule*, *SciPost Phys.* **9** (2020) 027, [`2007.01654`].

[94] C. M. Carloni Calame, M. Chiesa, S. M. Hasan, G. Montagna, O. Nicrosini and F. Piccinini, *Towards muon-electron scattering at NNLO*, *JHEP* **11** (2020) 028, [`2007.01586`].

[95] E. Budassi, C. M. Carloni Calame, M. Chiesa, C. L. Del Pio, S. M. Hasan, G. Montagna, O. Nicrosini and F. Piccinini, *NNLO virtual and real leptonic corrections to muon-electron scattering*, *JHEP* **11** (2021) 098, [`2109.14606`].

[96] R. Aliberti et al., *Radiative corrections and Monte Carlo tools for low-energy hadronic cross sections in e^+e^- collisions*, `2410.22882`.

[97] R. Bonciani et al., *Two-Loop Four-Fermion Scattering Amplitude in QED*, *Phys. Rev. Lett.* **128** (2022) 022002, [`2106.13179`].

[98] M. Delto, C. Duhr, L. Tancredi and Y. J. Zhu, *Two-Loop QED Corrections to the Scattering of Four Massive Leptons*, *Phys. Rev. Lett.* **132** (2024) 231904, [`2311.06385`].

[99] T. Becher and M. Neubert, *Infrared singularities of QCD amplitudes with massive partons*, *Phys. Rev. D* **79** (2009) 125004, [`0904.1021`].

[100] G. P. Korchemsky and A. V. Radyushkin, *Renormalization of the Wilson Loops Beyond the Leading Order*, *Nucl. Phys. B* **283** (1987) 342–364.

[101] T. Becher and M. Neubert, *Infrared singularities of scattering amplitudes in perturbative QCD*, *Phys. Rev. Lett.* **102** (2009) 162001, [`0901.0722`].

[102] A. Ferroglia, M. Neubert, B. D. Pecjak and L. L. Yang, *Two-loop divergences of massive scattering amplitudes in non-abelian gauge theories*, *JHEP* **11** (2009) 062, [`0908.3676`].

[103] A. Denner, G. Weiglein and S. Dittmaier, *Application of the background field method to the electroweak standard model*, *Nucl. Phys. B* **440** (1995) 95–128, [`hep-ph/9410338`].

[104] A. Denner and S. Dittmaier, *Electroweak Radiative Corrections for Collider Physics*, *Phys. Rept.* **864** (2020) 1–163, [`1912.06823`].

[105] S. Dittmaier, *Electric charge renormalization to all orders*, *Phys. Rev. D* **103** (2021) 053006, [`2101.05154`].

[106] S. Actis, A. Ferroglia, M. Passera and G. Passarino, *Two-Loop Renormalization in the Standard Model. Part I: Prolegomena*, *Nucl. Phys. B* **777** (2007) 1–34, [`hep-ph/0612122`].

[107] S. Actis and G. Passarino, *Two-Loop Renormalization in the Standard Model Part II: Renormalization Procedures and Computational Techniques*, *Nucl. Phys. B* **777** (2007) 35–99, [`hep-ph/0612123`].

[108] S. Actis and G. Passarino, *Two-Loop Renormalization in the Standard Model Part III: Renormalization Equations and their Solutions*, *Nucl. Phys. B* **777** (2007) 100–156, [`hep-ph/0612124`].

[109] G. Degrassi and A. Vicini, *Two loop renormalization of the electric charge in the standard model*, *Phys. Rev.* **D69** (2004) 073007, [`hep-ph/0307122`].

[110] T. Hahn, *Generating Feynman diagrams and amplitudes with FeynArts 3*, *Comput. Phys. Commun.* **140** (2001) 418–431, [`hep-ph/0012260`].

[111] P. Maierhöfer, J. Usovitsch and P. Uwer, *Kira—A Feynman integral reduction program*, *Comput. Phys. Commun.* **230** (2018) 99–112, [`1705.05610`].

[112] J. Klappert, F. Lange, P. Maierhöfer and J. Usovitsch, *Integral reduction with Kira 2.0 and finite field methods*, *Comput. Phys. Commun.* **266** (2021) 108024, [`2008.06494`].

[113] J. Klappert and F. Lange, *Reconstructing rational functions with FireFly*, *Comput. Phys. Commun.* **247** (2020) 106951, [`1904.00009`].

[114] F. Lange, J. Usovitsch and Z. Wu, *Kira 3: integral reduction with efficient seeding and optimized equation selection*, `2505.20197`.

[115] R. N. Lee, *LiteRed 1.4: a powerful tool for reduction of multiloop integrals*, *J. Phys. Conf. Ser.* **523** (2014) 012059, [`1310.1145`].

[116] A. von Manteuffel and C. Studerus, *Reduze 2 - Distributed Feynman Integral Reduction*, `1201.4330`.

[117] C. Meyer, *Algorithmic transformation of multi-loop master integrals to a canonical basis with CANONICA*, *Comput. Phys. Commun.* **222** (2018) 295–312, [`1705.06252`].

[118] R. N. Lee, *Libra: A package for transformation of differential systems for multiloop integrals*, *Comput. Phys. Commun.* **267** (2021) 108058, [`2012.00279`].

[119] A. Blondel, J. Gluza, S. Jadach, P. Janot and T. Riemann, eds., *Theory for the FCC-ee: Report on the 11th FCC-ee Workshop Theory and Experiments*, vol. 3/2020 of *CERN Yellow Reports: Monographs*, (Geneva), CERN, 5, 2019. 10.23731/CYRM-2020-003.